Development/Plasticity/Repair

Activity-Dependent Plasticity of Transmitter Release from Nerve Terminals in Rat Fast and Slow Muscles

Brian Reid,[1]* Vladimir N. Martinov,[2]* Arild Njå,[2] Terje Lømo,[2] and Guy S. Bewick[1]

[1]Department of Biomedical Sciences, Institute of Medical Sciences, University of Aberdeen, Aberdeen AB25 2ZD, United Kingdom, and [2]Department of Physiology, Institute of Basic Medical Sciences, University of Oslo, N-0317 Oslo, Norway

Neuromuscular junctions (NMJs) on fast and slow muscle fibers display different transmitter release characteristics that appear well adapted to the different patterns of nerve impulses that they transmit *in vivo*. Here, we ask whether the release properties of such NMJs, termed fast and slow, can be transformed by chronic nerve stimulation. In young adult rats, nerve impulse conduction in the sciatic nerve was blocked by TTX, and the nerve to the fast extensor digitorum longus (EDL) or the slow soleus (SOL) muscle stimulated directly below the block with slow (20 Hz for 10 sec every 30 sec) or fast (150 Hz for 1 sec every 60 sec) stimulus patterns, respectively. After 3–4 weeks, originally fast EDL-NMJs and slow SOL-NMJs had become almost fully transformed to slow and fast NMJs, respectively, with respect to maintenance of transmitter release during tonic 20 Hz stimulation *in vitro* and ratio of quantal content to vesicle pool size. TTX block alone had no such transforming effect. Vesicle recycle time was unaffected by the stimulation, whereas initial quantal content and vesicle pool size were reduced (by 49% and 57% in EDL and 33% and 67% in SOL). Muscle fiber diameter also declined (by 49% in EDL and 33% in SOL vs 46% in unstimulated SOL; unstimulated EDL was not examined). We conclude that fast and slow NMJs display marked plasticity by being able to adapt important release characteristics to the impulse patterns imposed on them.

Key words: **neuromuscular junction; synaptic plasticity; transmitter release; synaptic vesicles; rat; neural activity; FM1-43; stimulation; *in vivo***

Introduction

Neuromuscular junctions (NMJs) transmit impulses with high fidelity with the result that every presynaptic action potential elicits a postsynaptic action potential after a brief synaptic delay. Such fidelity exists at NMJs in both rapidly contracting (fast) and slowly contracting (slow) muscles despite the strikingly different impulse patterns that NMJs in such muscles normally transmit. For example, in rats moving unrestrained in their cages, motor neurons (MNs) to the fast extensor digitorum longus (EDL) muscle generate only a few thousand impulses per day in brief bursts at high frequency (~100 Hz), whereas MNs to the slow soleus (SOL) muscle generate several hundred thousand impulses per day, often in long trains at low frequency (~20 Hz) (Hennig and Lømo, 1985). For simplicity, we will refer here to MNs innervating fast and slow muscle fibers as fast and slow MNs delivering fast and slow impulse patterns to fast and slow NMJs.

NMJs that transmit such diverse impulse patterns differ structurally and functionally. In adult mice or rats, NMJs in slow SOL muscles display fewer terminal swellings (varicosities) (Wærhaug, 1992), more extensive and protruding primary clefts (Fahim et al., 1984), and weaker postsynaptic responses to given doses of acetylcholine (ACh) (Sterz et al., 1983) than NMJs in fast EDL muscles. During tonic stimulation, SOL-NMJs maintain vesicle release better than EDL-NMJs (Reid et al., 1999) and, in tibialis anterior muscles, slow NMJs are much more fatigue resistant than fast NMJs (Kugelberg and Lindegren, 1979).

Here, we ask whether NMJs in SOL and EDL of adult rats are also plastic. When forced to transmit slow or fast impulse patterns, will originally fast and slow NMJs acquire slow and fast properties, respectively? Such plasticity has been well established for fast and slow muscle fibers, the contractile properties of which undergo striking changes in slow or fast directions after cross-reinnervation (Close, 1969) or appropriate direct electrical muscle stimulation (Lømo et al., 1974; Eken and Gundersen, 1988; Ausoni et al., 1990; Windisch et al., 1998). Substantial synaptic plasticity has been observed in crayfish, in which the physiology and morphology of phasic NMJs become tonic-like after long-term tonic stimulation of their axons (Lnenicka and Atwood, 1985; Lnenicka et al., 1986). In rats, the nerve to EDL has been stimulated tonically at 10 Hz for 3–4 months with only a modest slowing effect on motor nerve terminal morphology, perhaps because the EDL-MNs continued to generate and conduct fast activity (Wærhaug and Lømo, 1994). Any effect of fast pattern activity on slow NMJs has not been reported so far for any system.

In the present experiments, we blocked impulse conduction in the sciatic nerve with TTX for 3–4 weeks and stimulated the nerves to EDL or SOL below the block with slow or fast electrical stimulus patterns. We then examined some key synaptic proper-

Received Feb. 21, 2003; revised Aug. 18, 2003; accepted Aug. 26, 2003.

This work was supported by the Wellcome Trust, European Union Biotechnology Programme (BIO CT96 0216, BIO CT96 0433), the Jahre Foundation, and the Norwegian Research Council. We thank Sigrid Shaller, Eva Aaboen Hanssen, and Bjarne Authen for excellent technical assistance and Sabiha Jawaid for fiber diameter data.

*B.R. and V.N.M. contributed equally to this work.

Correspondence should be addressed to Dr. Guy S. Bewick, Department of Biomedical Sciences, Institute of Medical Sciences, University of Aberdeen, Aberdeen AB25 2ZD, UK. E-mail: g.s.bewick@abdn.ac.uk.

Copyright © 2003 Society for Neuroscience 0270-6474/03/239340-09$15.00/0

ties of the NMJs and found that NMJs in EDL had undergone almost complete fast to slow, and NMJs in SOL similarly substantial slow to fast, transformation.

Materials and Methods

Animals. Adult male Wistar rats weighing 300–400 gm were used (B&K Universal, Sollentuna, Sweden). All surgical operations were performed under deep anesthesia with Equithesin (42.5 mg/ml chloral hydrate plus 9.7 mg/ml pentobarbitone; 0.4 ml/100 gm body weight, injected intraperitoneally). Temgesic (0.03 mg/100 gm body weight) was used for postoperative analgesia. The animals were kept in an animal facility under professional supervision and had *ad libitum* access to food and water. The experiments were approved by the Norwegian Animal Research Authority in accordance with Animal Protection Act of Norway.

Chronic nerve stimulation below a TTX block. Under surgical anesthesia, a capillary for slow release of TTX was inserted under the epineurium of the sciatic nerve between the diverging tibial, common peroneal, and sural nerves (Mills and Bray, 1979; Tsujimoto and Kuno, 1988) (Fig. 1*A*). A soft cuff of silicone rubber was placed around the nerve to limit the escape of TTX and to raise its concentration in the nerve (Pasino et al., 1996). Electrodes were then implanted either near the common peroneal nerve (Windisch et al., 1998) or near the SOL nerve. In some animals, we blocked the nerve with TTX but did not implant any electrodes for stimulation. The TTX capillary was 10 mm long and made from borosilicate glass [inner diameter (ID), 1.12 mm; outer diameter, 1.50 mm). Its tapered end was fire-polished to an ID of 28–30 μm, and the other end was fire-polished to an ID of ~500 μm. The capillary was filled with 30 mM TTX in citrate buffer (Alomone Labs, Jerusalem, Israel) and sealed at its blunt end with a silicone sealant. The internal volume of the capillary was larger than that described in previous reports (5 μl compared with only 0.5–1 μl), and the duration of the block was longer (4–6 weeks compared with only 6–10 d) (Mills and Bray, 1979; Tsujimoto and Kuno, 1988). Normal function returned within 1–2 d if the capillary was removed. The conduction block was tested daily by the toe spreading reflex, by the withdrawal reflex to a skin pinch on the lateral aspect of the foot, and, under surgical anesthesia, by electrical stimulation of the nerve above and below the block before removing the muscle for the acute experiment. The main advantage of implanting a capillary instead of an osmotic minipump (Pasino et al., 1996) as a source of TTX is that it requires less space and less surgical intervention, whereas the efficiencies of the two methods seem to be the same.

The implanted electrodes were flexible miniature insulated medical wire (catalog #AS 632; Cooner Wire, Inc., Chatsworth, CA) placed parallel to the nerve and ~2 mm away from it. For stimulation of the SOL nerve, the wires were pulled underneath and through parts of the gastrocnemius muscle that cover the SOL nerve, using a 23 gauge cannula as guide. For anchoring, small knots were tied in the wire flanking a 3-mm-long segment where the insulation was removed. Sutures (7.0 silk) for fixing the wire to adjacent tissue were placed more proximally, near an additional knot in the wire. A thin layer of the gastrocnemius muscle covered the cut ends of the wires and prevented them from touching the SOL nerve and muscle (Fig. 1*A*). Stimulation of the common peroneal nerve was essentially as described by Windisch et al. (1998). However, to prevent electrode breaks, the stimulating wires were exposed for 3 mm near the tip by removing insulation from approximately one-half of the circumference, leaving the remaining insulation in continuity as mechanical support for the exposed metal strands. The stimulating current delivered through the implanted electrodes was monitored daily by the potential drop (on an oscilloscope screen) across a 100 Ω series resistor and adjusted to ~1.5 times the intensity necessary for maximum palpable contraction in the innervated muscle group, usually 0.5–1.5 mA. The "fast pattern" of stimulation delivered to the SOL nerve consisted of 150 square pulses at 150 Hz every 60 sec (i.e., 1 sec of high-frequency activity/min), whereas the "slow pattern" delivered to the peroneal nerve consisted of 200 pulses at 20 Hz every 30 sec (i.e., 20 sec of low-frequency activity/min). Each pulse was bipolar and 0.2 msec long in each direction. The electrical connections to the stimulator, which allowed the rat to move relatively freely in its cage with *ad libitum* access to food and water, were as described by Windisch et al. (1998). Some animals were killed early and not used because of suspected systemic TTX overload ($n = 7$) or a skin wound on the anesthetized foot ($n = 2$). Accordingly, the data we report here are exclusively from animals maintaining good health and fully functional implants throughout ($n = 50$; 21–34 d; mean, 27 d).

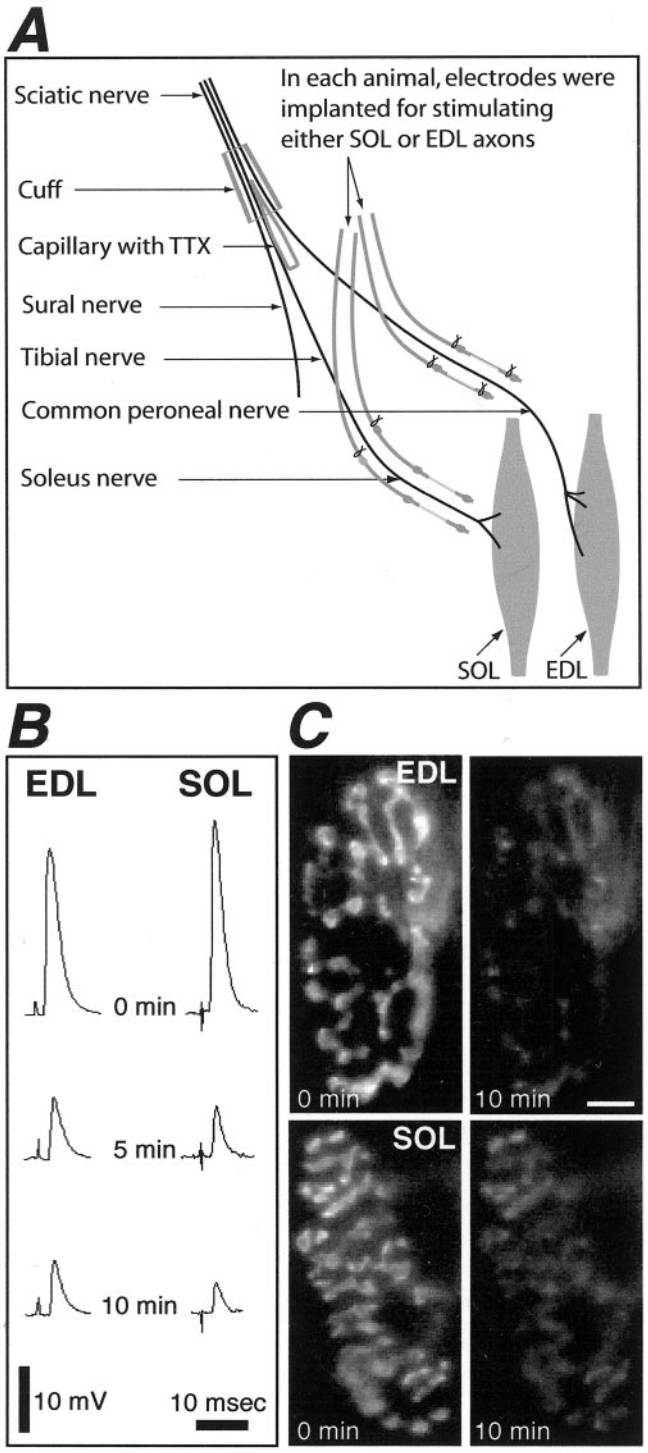

Figure 1. Surgical paradigm, intracellular recording, and fluorescent imaging. *A*, Diagram showing placement of TTX capillary for blockade of impulse conduction and electrodes for electrical stimulation below the block. EPPs (*B*) and FM1-43 (*C*) fluorescence in motor nerve terminals during continuous nerve stimulation at 20 Hz *in vitro*. The muscles in *B* and *C* had been removed after chronic nerve stimulation *in vivo*. The nerve to the fast EDL muscle had been stimulated for 3–4 weeks with a slow pattern, whereas the nerve to the slow SOL muscle had been stimulated for 3–4 weeks with a fast pattern. See Materials and Methods for additional details. Scale bar: *C*, 10 μm.

Destaining and electrophysiology. After 21–34 d of stimulation, SOL or EDL muscles with nerves attached were dissected out under anesthesia and pinned out on Sylgard (Dow Corning, Wiesbaden, Germany) in a 55 mm dish containing Liley's saline (1956) gassed with 95% O_2 and 5% CO_2. Liley's saline contains (in mM): 138.8 NaCl, 12 $NaHCO_3$, 4 KCl, 1 KH_2PO_4, 1 $MgCl_2$, 2 $CaCl_2$, and 11 glucose. To label synaptic vesicles, muscles were (1) soaked for 20 min in 1 μM FM1-43 (Molecular Probes, Eugene, OR), (2) stimulated via a suction electrode on the nerve for 15 min with alternating trains of 10 Hz for 10 sec and 1 Hz for 5 sec, and (3) washed in fresh gassed dye-free saline for 30 min to remove any dye not internalized. To prevent contraction during imaging and intracellular recording, labeled preparations were soaked in 2 μM μ-conotoxin GIIIB (Scientific Marketing Associates, Barnet, UK) for 60–90 min. At this concentration, μ-conotoxin GIIIB selectively blocks voltage-gated sodium channels (and, hence, excitation–contraction coupling) in rat skeletal muscle, whereas neural sodium channels and neuromuscular transmission are unaffected (Plomp et al., 1992). Muscles that had been chronically paralyzed *in vivo* without stimulation, however, became resistant to conotoxin. We were able to block contraction completely and obtain satisfactory recordings using the cut-fiber procedure (Barstad, 1962) in SOL, but this was unsuccessful in EDL muscles.

Labeled terminals were illuminated with a 100 W mercury arc lamp, attenuated with neutral density filters to 1.5% of maximum intensity to prevent excessive bleaching and phototoxicity. Images were acquired using a Photonic Science (Robertsbridge, UK) Mono Coolview charge-coupled device camera, via an Olympus LUM Plan Fl 40× water immersion lens (0.8 numerical aperture) and saved onto an Apple Power Macintosh 6500/275 computer running Openlab software (version 2.1.1; Improvision, Coventry, UK). Sharp glass microelectrodes containing 3 M KCl were used to record miniature endplate potentials (MEPPs) from fibers of which terminals were imaged. The data were recorded via a Biologic (Claix, France) VF 180 amplifier onto Biologic digital audio tape and a Longshine personal computer using Strathclyde Electrophysiology Software Whole Cell Program (WCP version 1.2; provided by John Dempster, Department of Physiology and Pharmacology, University of Strathclyde, Glasgow, UK). Images and endplate potentials (EPPs) were collected simultaneously during stimulation of the muscle at 20 Hz for 10 min. Typical terminal destaining and EPP rundowns from this procedure are shown in Figure 1, *B* and *C*. Muscle fibers displaying failures on nerve stimulation or complete rundown of EPPs within the first 2 min were rejected. All experiments were performed at room temperature (18–22°C).

Images were analyzed using NIH Image 1.62. The first image (time 0) was enhanced for contrast (this does not change the brightness values measured), and all labeled, in-focus boutons were outlined manually using the freehand region of interest (ROI) tool (Reid et al., 1999, their Fig. 4). A rectangular background ROI was also selected near the terminal for background-subtraction of the terminal ROI values. This terminal/background ROI mask was then used to analyze the remaining images in the time series. Although bouton and terminal shape do not change during destaining, the mask was manually realigned to compensate for any drift in X or Y position of the terminal during destaining. The decline in staining intensity was expressed as a percentage, taking the initial intensity as 0% dye lost and the intensity after 10 min of stimulation as 100% dye lost (see Fig. 4). MEPPs and EPPs were analyzed using WCP for Windows (WinWCP version 3.0.6). Quantal content (QC) was determined by the direct method and corrected for nonlinear summation, using the formula: $QC = E \div [M \times (1 - (E \div Vm))]$, where E is the amplitude of the first EPP of the train and M is the mean MEPP amplitude. The original Martin (1955) correction for nonlinear summation was used to allow direct comparison with the data from normal muscles in the previous study (Reid et al., 1999). This formula leads to a slight overestimate of QC (and vesicle pool size; see Results) compared with the later, revised formula (McLachlan and Martin, 1981). Because much of the data are normalized to internal controls (i.e., rundowns are expressed as percentage of initial values), this technique is valid for such a comparative study. Furthermore, the differences are small (in comparative calculations, differences were found to be <10% for QC and <5% for vesicle pool size) and similar in each preparation group. The advantage of direct comparison with the normal control data of the previous study more than compensates for the small differences introduced by continued use of the older formula and has no effect on the conclusions drawn. Recycle time (RT) was determined from plots of relative dye loss and cumulative QC, scaled to overlap as long as possible from time 0 (see Fig. 4). The time to deviation of the two curves, when recycled vesicles emptied of dye first begin to be released again, can then be taken as the vesicle RT (Betz and Bewick, 1993).

Vesicle pool size was calculated at the RT for each terminal, as: $VP = (100 \div \text{dye loss}_{RT}) \times (QC_{RT})$, where VP is the vesicle pool size, dye loss_{RT} is percentage of dye lost from start of stimulation to the RT, and QC_{RT} is the cumulative total of quantal release at the RT. Previous control experiments in unoperated preparations (Reid et al., 1999) had established that these estimates agreed with other measures of mammalian vesicle pool size in normal muscles and that all terminals were fully loaded with dye by the loading regime (Betz and Bewick, 1992, 1993; Reid et al., 1999).

Statistics. Data are shown as mean ± SEM. Data from unstimulated muscles are derived from the previous study of normal muscles (Reid et al., 1999), except for the initial terminal fluorescence values (see Fig. 5*C*). These were derived from a new cohort of preparations processed and imaged identically in parallel with the experimental muscles to facilitate a direct comparison. Differences between mean values were compared using a two-sample Student's *t* test, performed with equal or unequal variance according to an *f* test.

Results

Effects on QC

QC rundown

After 3–4 weeks of chronic stimulation *in vivo*, SOL or EDL muscles were removed from the animal and stimulated *in vitro* at 20 Hz for 10 min while recording EPPs. QC of the first recorded EPP was calculated by the direct method (see Materials and Methods) and set at 100%, and that of subsequent EPPs was plotted as a percentage of the first (Fig. 2). Normally, QC declines faster and reaches lower values in EDL than in SOL (Reid et al., 1999). However, for EDL preparations chronically stimulated with a slow pattern, the decline in QC was substantially transformed toward that of normal SOL (Fig. 2*A*). Conversely, the decline in SOL preparations that had received fast pattern stimulation was substantially transformed toward that of normal EDL (Fig. 2*B*). This pattern of transformation is also seen in the rates of EPP amplitude rundown for stimulated EDL and SOL (Fig. 1*B*). In contrast, SOL preparations that had been exposed to nerve conduction block without stimulation for the same length of time showed no transformation and maintained release to the same extent as normal SOL terminals (Fig. 2*C*). Unfortunately, we were unable to examine chronically inactive EDL preparations in the same way (see Materials and Methods). It is interesting to note that both SOL and EDL preparations exposed to nerve conduction block without stimulation became resistant to μ-conotoxin GIIIB. Such conotoxin-resistant muscle action potentials did not occur in stimulated preparations, providing further evidence that the chronic stimulation had been effective. Closer inspection of the QC rundown data revealed that the rundown was slower initially (0–2 min) and faster later on (2–10 min) in stimulated EDL compared with normal SOL and faster initially and slower later on in stimulated SOL compared with normal EDL, but these deviations were modest. Accordingly, in terms of QC rundown, NMJs in EDL and SOL underwent essentially complete fast to slow and slow to fast transformation, respectively, during long-term nerve stimulation.

Initial QC

Initial QC is higher in normal EDL than in normal SOL muscles (Gertler and Robbins, 1978; Wood and Slater, 1997; Reid et al.,

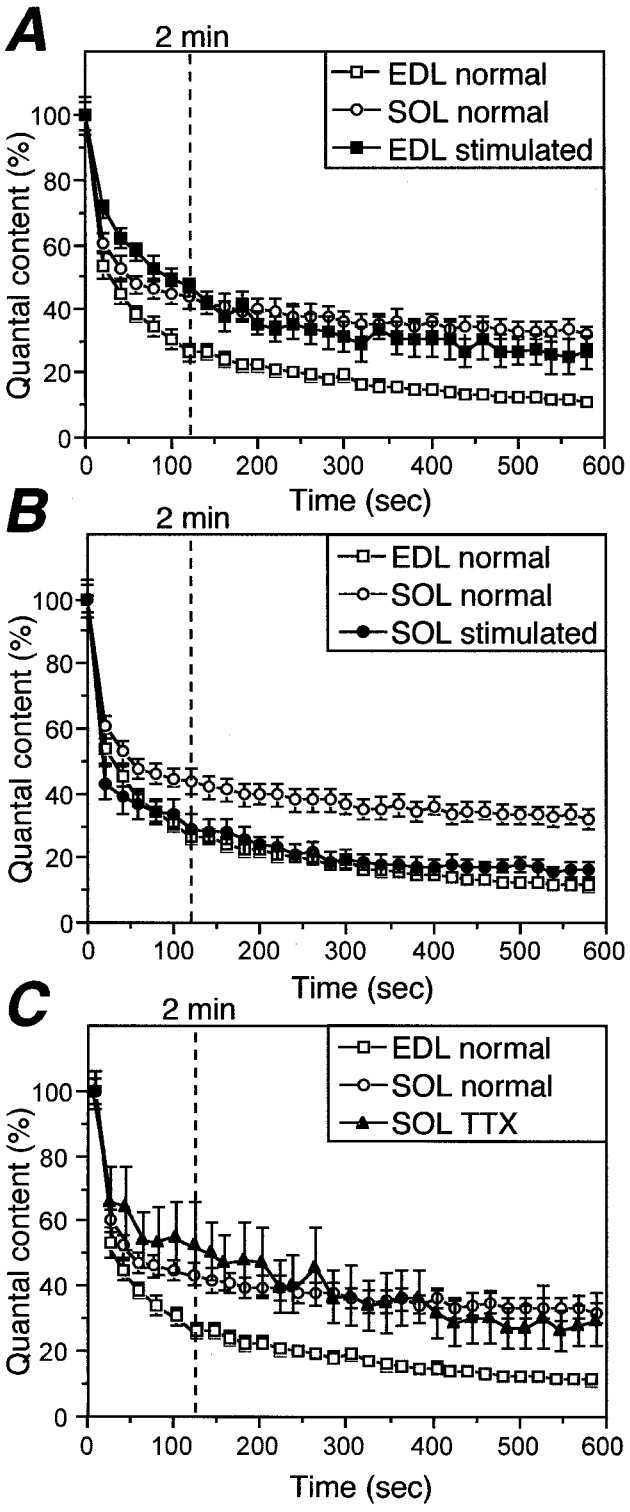

Figure 2. Activity pattern-dependent plasticity at stimulated fast and slow NMJs. *A*, Quantal content rundown at NMJs in fast EDL muscles that had been chronically stimulated *in vivo* with a slow stimulus pattern resembles rundown at normal SOL NMJs. The stimulations were applied to the nerves below a local TTX block for 3–4 weeks. The rundown was measured *in vitro* during 10 min of continuous stimulation at 20 Hz. *B*, Quantal content rundown at NMJs in slow SOL muscles that had been chronically stimulated *in vivo* with a fast stimulus pattern resembles normal EDL rundown. *C*, Quantal content rundown at NMJs in SOL muscles that had been blocked but had received no stimulation. Open symbols, Normal; filled symbols, stimulated; circles, EDL; squares, SOL; triangles, TTX-only SOL. Values are given as means ± SEM with $n = 10$ for each set of experiments, except stimulated EDL ($n = 8$) and TTX-only SOL ($n = 5$). Normal values are from Reid et al. (1999).

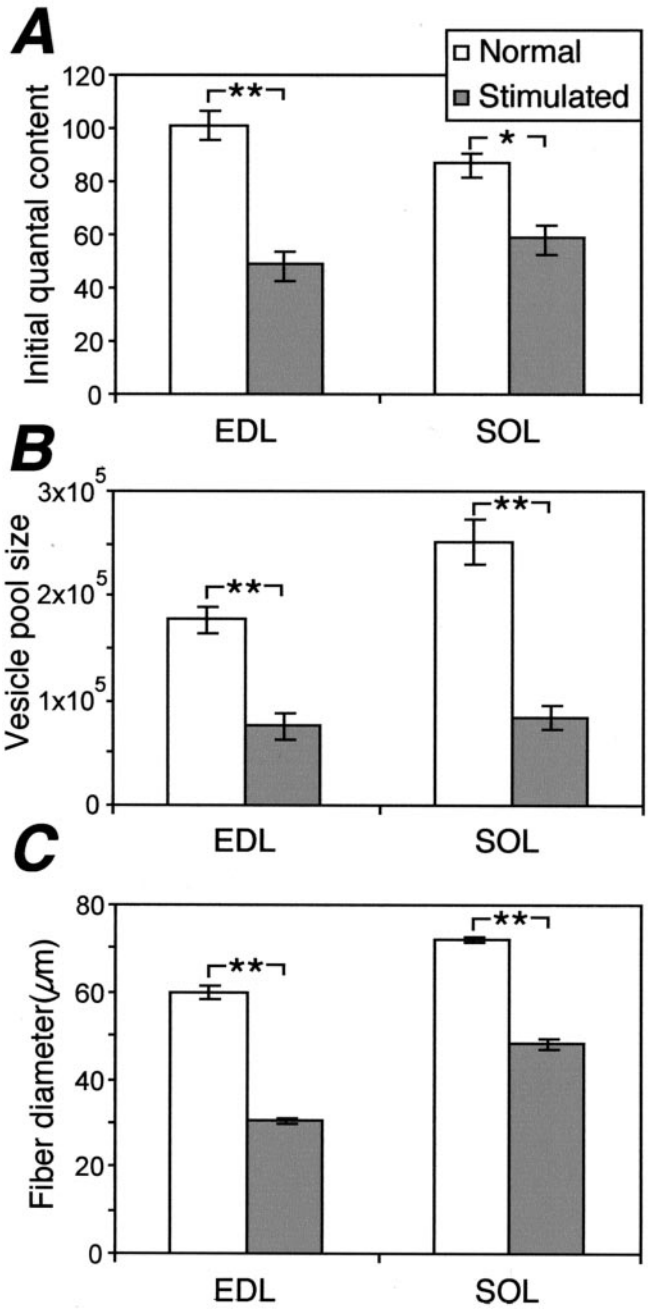

Figure 3. Chronic nerve stimulation causes reduction in initial quantal content, vesicle pool size, and fiber diameter. NMJs in fast EDL and slow SOL muscles had received slow and fast pattern stimulation, respectively, to their nerves below a local TTX block for 3–4 weeks. Note the similar reductions in initial quantal content (*A*), vesicle pool size (*B*), and fiber diameter (*C*), regardless of muscle type and fast or slow stimulus patterns. Open columns, normal; filled columns, stimulated. In *A–C*, $n = 24$, 7, and 74 for stimulated EDL and 18, 7, and 70 for stimulated SOL. *$p < 0.02$; **$p < 0.0001$. Normal values are from Reid et al. (1999) ($n = 10$), except normal fiber diameters are from Jawaid (2000) ($n = 180$ fibers from 6 muscles).

1999) (Fig. 3*A*). After the chronic nerve stimulations, initial QC became 33% lower than normal ($p < 0.02$) at NMJs in SOL muscles exposed to fast pattern activity and 54% lower than normal ($p < 0.0001$) at NMJs in EDL muscles exposed to slow pattern activity (Fig. 3*A*). Similar reductions occurred in muscle fiber diameter (Fig. 3*C*; see below), suggesting that the two processes were linked. Thus, as muscle fiber diameters decreased and their input resistance likely increased (Katz and Thesleff, 1957;

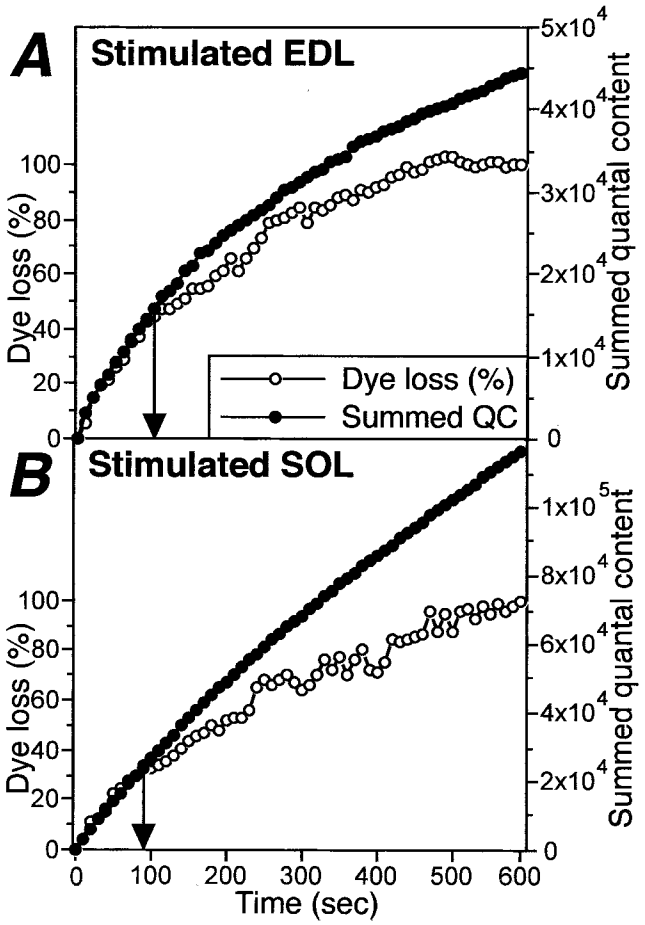

Figure 4. Estimation of vesicle pool size and vesicle RT in chronically stimulated NMJs. NMJs in fast EDL (*A*) and slow SOL muscles (*B*) had received slow and fast pattern stimulation, respectively, to their nerves below a TTX block for 3–4 weeks. Summed QC and relative loss of dye from FM1-43-loaded vesicles during continuous 20 Hz stimulation *in vitro* changed proportionally for approximately the first 100 sec and then diverged (arrows). Total vesicle pool size was determined at the point of divergence from the number of vesicles lost and the fraction of dye lost to that point (see Materials and Methods). Note that vesicle RT, taken as the time from onset to the point of divergence (see Materials and Methods), is similar at all NMJs, whether stimulated (*A*, *B*) or normal muscles (Table 1). Open circles, percentage of dye loss; filled circles, summed QC.

Barry and Ribchester, 1995), QC was downregulated proportionately, presumably because fewer quanta were now required to reach threshold for action potential generation (for review, see Wood and Slater, 2001, and references therein).

Effects on vesicle behavior

Vesicle pool size

Changes in the number of vesicles available for release (vesicle pool size) might contribute to stimulation-induced changes in QC rundown. To estimate vesicle pool size, we loaded the nerve terminals at EDL and SOL NMJs *in vitro* with fluorescent FM1-43 and monitored the dye loss and cumulative QC from the nerve terminal during stimulation at 20 Hz for 10 min (Reid et al., 1999). Initially, both dye loss and cumulative QC changed at the same rate (Fig. 4). During the first 90 sec of stimulation, the EDL NMJ shown in Figure 4*A* lost 43% of its fluorescence and 14,353 vesicles (summed QC at that point). Accordingly, the estimated initial vesicle pool size for this terminal was 33,379 (14,353 × 100/43; see Materials and Methods) (Reid et al., 1999). Similarly, the SOL NMJ in Figure 4*B* lost 29% of its fluorescence and 22,613 vesicles in 80 sec, resulting in an estimated vesicle pool size of 74,528. On average, the estimated vesicle pool size was similar in stimulated EDL and SOL ($n = 7$ for both) and much smaller than in normal muscles (47% and 37% of normal in EDL and SOL, respectively; both $n = 7$ and $p < 0.0001$) (Fig. 3*B*).

QC to vesicle pool size ratio

We next went on to explore how the relationship between QC and vesicle pool size had changed in the stimulated terminals. Initial QC is smaller, and vesicle pool size is larger, at NMJs in fatigue-resistant normal SOL compared with fatigue-sensitive normal EDL (Table 1 in Reid et al., 1999). Consequently, the ratio of initial QC to vesicle pool size (QC/VP) is also smaller at SOL compared with EDL-NMJs. We have proposed previously (Reid et al., 1999) that this might be the physiological basis enabling NMJs that are resistant to synaptic fatigue to maintain release (Kugelberg and Lindegren, 1979). Thus, synaptic fatigue might be prevented by releasing a small number of vesicles per impulse from a large vesicle pool. To test this hypothesis directly, the same analysis was, therefore, performed on the stimulated preparations (Fig. 5*A*). Like QC rundown (Fig. 2*A*,*B*), the QC/VP ratio underwent nearly complete fast to slow (EDL) or slow to fast (SOL) transformation after chronic stimulation. Accordingly, in the process of adapting to the impulse pattern imposed on them with respect to QC and vesicle pool size, these values seem to be adjusted to produce the appropriate QC/VP ratio for the activity pattern they experience.

Vesicle density and initial terminal fluorescence intensity

Clearly, the reductions in vesicle pool size described above are substantial. It might be expected, therefore, that labeled stimulated terminals would have a lower initial fluorescence intensity. The data were analyzed further to determine whether initial fluorescence intensity was reduced in stimulated terminals in proportion to the calculated reduction in vesicle pool size. Terminal fluorescence intensity, however, is not dependent simply on the number of vesicles, but rather their density (i.e., the number of fluorescent vesicles per unit terminal area). Because changes in activity can affect terminal morphology (Deschenes et al., 1993; Wærhaug and Lømo, 1994), it is important to use VP density to make this comparison. The results of this analysis revealed that there had been a large reduction in VP per unit terminal area (Fig. 5*B*) and that a similar reduction in initial terminal fluorescence was observed (Fig. 5*C*). There are no error bars in Figure 5*B* because these data are the ratio of mean values from two independent data sets, i.e., the calculated VP [$n = 10$ for normal muscles (Reid et al., 1999) and $n = 7$ for stimulated muscles] and the terminal area of *en face* terminals postlabeled with anti-synaptophysin, another vesicle label ($n = 55$–175 terminals, from at least five muscles in all cases).

Interestingly, although stimulation affected terminal morphology, total terminal area occupied by vesicles was not changed significantly. The full morphological changes induced by stimulation will be reported in detail elsewhere but, pertinent to the present study, a reduction in the lateral extent of the terminal arborization, presumably because of the decrease in fiber diameter, was offset by an increase in terminal extent along the long axis of the fiber. Thus, these data also show that the downregulation of initial QC and vesicle pool size in stimulated terminals occurs without a change in total terminal area occupied by vesicles.

Table 1. Effects of chronic nerve stimulation on other properties of NMJs

	SOL		EDL	
	Normal	Fast pattern stimulation	Normal	Slow pattern stimulation
Vesicle recycle time (sec)	119.0 ± 10.2* ($n = 10$; $p > 0.6$)	126.7 ± 18.1 ($n = 9$; $p > 0.1$)	109.6 ± 11.2* ($n = 10$; $p > 0.4$)	100.0 ± 7.6 ($n = 8$)
EPP rise time (msec)	1.68 ± 0.04 ($n = 41$; $p < 0.0008$)	1.18 ± 0.12 ($n = 18$; $p > 0.06$)	0.86 ± 0.04 ($n = 48$; $p > 0.1$)	0.93 ± 0.04 ($n = 24$)
EPP fall time (T_{50}) (msec)	2.85 ± 0.11 ($n = 41$; $p < 0.004$)	2.31 ± 0.14 ($n = 18$; $p < 0.007$)	2.10 ± 0.09 ($n = 48$; $p > 0.06$)	1.86 ± 0.07 ($n = 24$)
MEPP amplitude (mV)	0.28 ± 0.02* ($n = 10$; $p < 0.0001$)	0.55 ± 0.04 ($n = 18$; $p > 0.7$)	0.28 ± 0.01* ($n = 10$; $p < 0.0001$)	0.50 ± 0.05 ($n = 24$)
MEPP frequency (MEPPs/sec)	3.0 ± 0.7* ($n = 10$; $p > 0.08$)	1.9 ± 0.4 ($n = 18$; $p > 0.4$)	2.7 ± 0.4* ($n = 10$; $p > 0.2$)	2.2 ± 0.4 ($n = 24$)

NMJs in fast EDL and slow SOL muscles had received slow and fast pattern stimulation, respectively, to their nerves below a local TTX block for 3–4 weeks. Values are mean ± SEM. Probability values represent a Student's *t* test performed for samples of equal or unequal variance according to a preceding *f* test. Probability values in the normal columns show comparison between control and stimulated muscles. Probability values in the stimulated SOL column show comparison with stimulated EDL. *Data from Reid et al. (1999).

Vesicle RT

An alternative (or additional) way to sustain neurotransmitter release during repetitive activation would be to recycle vesicles more quickly. Vesicle RT can be estimated by comparing the curves for dye and vesicle loss (Betz and Bewick, 1992; Reid et al., 1999). In normal muscles, these curves deviate after ~100 sec of stimulation. Such deviation occurs when vesicles that have unloaded their FM1-43 by exocytosis at the onset of stimulation are recovered and undergo a second exocytosis without dye loss (Reid et al., 1999). In chronically stimulated terminals, using the same methods, we found that the RT (Table 1) was similar to that described previously for normal NMJs in both EDL and SOL (Reid et al., 1999). Accordingly, vesicle RT measured under these conditions is a relatively constant feature of motor nerve terminals, whether fast or slow, stimulated or unstimulated; it is unaffected by differences in transmitted impulse patterns.

Postsynaptic effects

Fiber diameter

Muscle paralysis by TTX alone resulted in considerable muscle atrophy, because mean fiber diameter in SOL decreased from 72.2 ± 0.6 μm in control muscles ($n = 180$; six muscles) (Jawaid, 2000) to 39.0 ± 1.5 μm ($n = 44$; two muscles) (Fig. 3*C*). Chronic stimulation counteracted part of this atrophy because the SOL fibers at the end of chronic stimulation had a mean diameter of 48.4 ± 1.3 μm ($n = 70$; two muscles; $p \leq 0.0001$ compared with unstimulated muscles). Similarly, the mean fiber diameter was smaller in stimulated EDL (30.3 ± 0.7 μm; $n = 74$; two muscles) than in normal EDL (59.9 ± 1.5 μm; $n = 180$; six muscles) (Jawaid, 2000) (Fig. 3*C*). Paralyzed and unstimulated EDL was not examined (see Materials and Methods).

Endplate potentials

In normal adult rats, nerve-evoked EPPs are faster in EDL than in SOL, in terms of both rise time and time to fall to 50% of peak amplitude (T_{50}) (Wood and Slater, 1997; Reid et al., 1999). These parameters were, therefore, examined for effects in the stimulated preparations (Table 1). Chronic stimulation had no obvious effect on either parameter at NMJs in EDL. In contrast, both values became smaller in stimulated SOL (Table 1). Many factors affect the time course of EPPs, including the degree of asynchronous presynaptic transmitter release, rate of ACh hydrolysis by ACh-esterase in the synaptic cleft, as well as distribution and kinetics of postsynaptic ACh receptors (AChRs). The present data do not distinguish between these possibilities.

MEPPs

MEPPs recorded in normal SOL and EDL muscles are similar in amplitude and frequency (Wood and Slater, 1997; Reid et al., 1999). After chronic stimulation, the amplitude increased and the frequency decreased in both SOL and EDL (Table 1). The increase in MEPP amplitude may be attributed, at least in part, to the muscle fiber atrophy and accompanying increase in input resistance.

Discussion

The present results show that chronic nerve stimulation with appropriate stimulus patterns can transform fast and slow NMJs into slow and fast NMJs, respectively. Slow pattern stimulation caused NMJs in fast EDL to become nearly as slow as NMJs in normal SOL with respect to ratio of QC over vesicle pool size and QC rundown during repetitive impulse activity. Conversely, fast pattern stimulation caused NMJs in SOL to become nearly as fast as NMJs in normal EDL. Vesicle RT, which is similar in normal SOL and EDL, was not changed. It seems, therefore, that the rate of QC rundown is positively correlated with, and perhaps determined by, the ratio of QC over vesicle pool size, ensuring the ability of NMJs to maintain transmitter release during continued activity as normally generated by slow MNs. The observed transformations of transmitter release properties are, therefore, clearly adaptive and in agreement with the higher resistance to fatigue at slow NMJs compared with fast NMJs reported by Kugelberg and Lindegren (1979). Moreover, the transformations appear analogous to the transformations of contractile properties of fast and slow muscle fibers induced by cross-reinnervation (Close, 1969) or appropriate activation of fast and slow muscles by electrical nerve (Salmons and Vrbova, 1969) or muscle (Lømo et al., 1974; Eken and Gundersen, 1988; Windisch et al., 1998) stimulation.

Inactivation of NMJs and muscle fibers by TTX in unstimulated preparations had no transforming effect on transmitter release characteristics. Such inactivation causes the appearance of extrajunctional AChRs (Cangiano and Lutzemberger, 1980) as well as TTX-resistant (Cangiano and Lutzemberger, 1980) and μ-conotoxin-resistant (the present study) action potentials in muscle fibers. Therefore, to eliminate stimulation-induced contractions during recording, we cut the muscles on each side of their endplate bands (Barstad, 1962) and succeeded in immobilizing SOL but not EDL muscles. Accordingly, data on the effects of TTX treatment alone are restricted to SOL-NMJs. However, the presence of μ-conotoxin-resistant muscle action potentials in only unstimulated TTX preparations shows that our chronic stimulations were effective, just as direct muscle stimulation blocks the expression of TTX-resistant voltage-gated sodium channels and extrajunctional AChRs in muscles inactivated by denervation (Lømo and Rosenthal, 1972; Awad et al., 2001).

Chronic stimulation counteracted some, but not all, of the fiber atrophy caused by TTX treatment alone. The remaining atrophy we attribute in part to the paralyzing effect of TTX on antagonistic unstimulated muscles, which reduced the load on the EDL and SOL during the stimulation. This effect may be compared with tenotomy, which causes severe atrophy, although the tenotomized fibers continue to be active and display normal sensitivity to ACh (Lømo and Rosenthal, 1972). In EDL, the

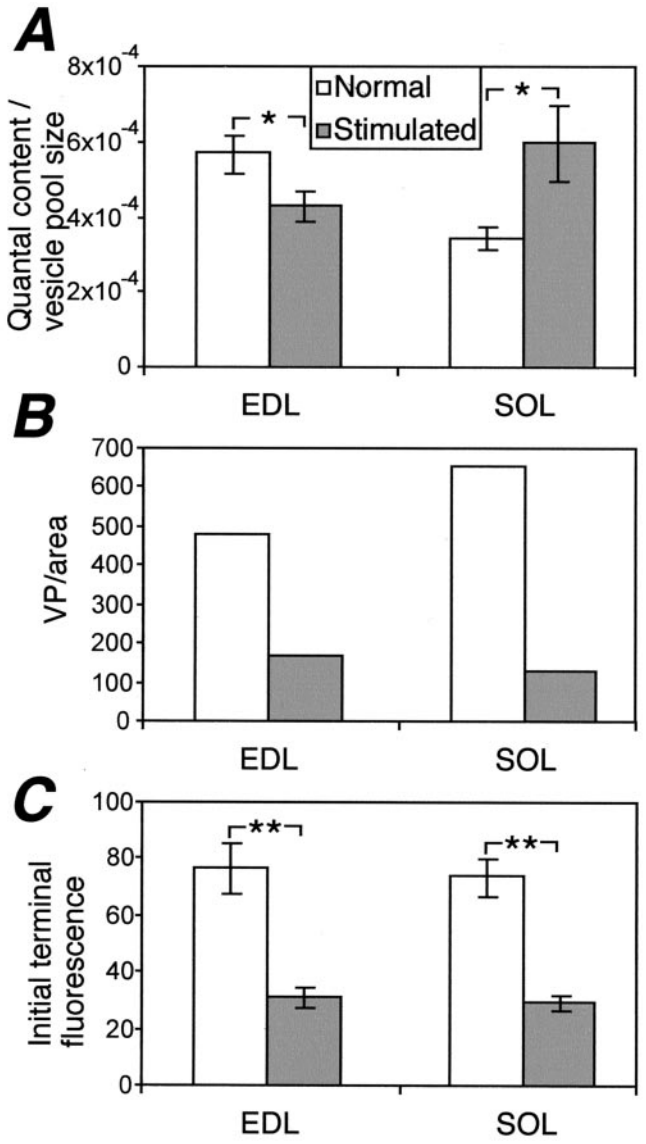

Figure 5. *A*, Transformation of the ratio of quantal content to vesicle pool size at chronically stimulated NMJs. NMJs in fast EDL and slow SOL muscles received slow and fast pattern stimulation, respectively, to their nerves below a TTX block for 3–4 weeks, and estimates of quantal content and vesicle pool size were determined (see Materials and Methods). The ratio of quantal content to vesicle pool size increased in stimulated SOL, becoming not significantly different from the ratio at normal EDL. Conversely, this ratio in stimulated EDL had decreased significantly toward the value found at normal SOL. Open columns, Normal; filled columns, stimulated. The values for stimulated muscles are mean ± SEM ($n = 7$). *$p < 0.04$. Normal values are from Reid et al. (1999) ($n = 10$). *B*, The ratio of VP size to terminal area was much lower in stimulated muscles, because VP was substantially reduced but terminal areas were unchanged from normal muscles. There are no error bars because the VP/area ratios are derived from the means of two sets of independent data (see Results). *C*, Initial terminal fluorescence (measured by FM1-43 labeling) was also lower, consistent with a lower vesicle density in the stimulated terminals. Stimulated EDL, $n = 37$; stimulated SOL, $n = 29$. **$p < 0.0001$.

smaller than normal fiber diameter may also reflect an adaptation to the imposed tonic activity, because large amounts of chronic low-frequency stimulation induce progressively smaller muscle fibers, particularly in initially large type 2B fibers but not type 1 fibers (Delp and Pette, 1994), presumably because the decreased fiber diameter facilitates oxygen diffusion into the center of the fibers (Salmons and Henriksson, 1981). Such tonic stimulation also reduces tetanic force output more than much smaller amounts of phasic stimulation (Kernell et al., 1987; Westgaard and Lømo, 1988). Finally, we hardly expected to find "normal" fiber diameters in the present experiments, given the artificial nature of the imposed muscle use and the strong use-dependent variability of fiber diameter in normal muscle.

As mentioned, transformation of synaptic properties occurred when the fast EDL and slow SOL nerves were stimulated below the TTX block with opposite patterns. We would have liked to see that "normal" control patterns maintain normal synaptic properties but decided against this experiment because of the relatively expensive and large amount of work involved. Furthermore, because such opposite patterns induce marked transformation of contractile properties in EDL and SOL, whereas control patterns maintain normal fast and slow properties (Eken and Gundersen, 1988; Gorza et al., 1988), significant transformation by control, endogeneous-like patterns seems very unlikely. Accordingly, we conclude that the observed transformation of synaptic properties was determined entirely or primarily by the imposed fast or slow activity patterns.

In the present experiments, the TTX block prevented impulses generated in the periphery from reaching the spinal cord. Consequently, the transformation of NMJ properties did not depend on activity-related depolarization of cell bodies, as has been reported for crayfish NMJs (Hong and Lnenicka, 1993, 1995). Instead, local processes at individual NMJs, acting independently of processes occurring in the cell body, might have been responsible. This possibility is suggested by studies on cultured rat sympathetic neurons (Campenot, 1994; Campenot and Eng, 2000). Furthermore, in nerve–muscle cultures from *Xenopus*, neurotrophin-4 (NT4) causes rapid potentiation of synaptic transmission through processes that are spatially restricted to <60 μm from the site of NT4 presentation (Wang et al., 1998).

Whether the observed transformations required interaction with the muscle fiber, for example in the form of muscle activity-dependent retrograde signals, is not known. Such signals may reach MNs in the spinal cord even in the presence of nerve blocks by TTX. For example, SOL MNs in the cat acquire shorter afterhyperpolarizations (AHPs) when exposed to disuse by spinal cord transection. This change is prevented by *in vivo* stimulation of SOL axons below, but not above, a TTX block. Only slow pattern stimulation (10 Hz) maintains slow AHPs in disused SOL MNs, because a relatively fast pattern (50 Hz) is without this effect (Czeh et al., 1978). Candidates for activity-dependent retrograde trophic signals from muscle include the neurotrophins NT4 and BDNF. NT4 synthesis in muscle is regulated by synaptic activity and modulates the efficiency of transmission at NMJs (Funakoshi et al., 1995; Wang et al., 1998). However, the expression of trkB (a receptor for NT4 and BDNF) is not detectably different in fast and slow MNs (Copray and Kernell, 2000). Conversely, some properties of motor nerve terminals can be transformed in the absence of muscle fibers. For example, Ca^{2+} clearance in phasic axons growing from crayfish nerve cord explants is very slow, but after 5 d of tonic stimulation it accelerates to a level comparable with that in tonic axons (Lnenicka et al., 1998; Fengler and Lnenicka, 2002). In rats, the contribution of muscle-derived, activity-dependent signaling to the synaptic plasticity observed here might be tested by blocking postsynaptic activity chronically with α-bungarotoxin, using an experimental protocol like the one for the present study.

Interestingly, transformed EDL-NMJs and SOL-NMJs did not become identical to normal SOL-NMJs and EDL-NMJs. With respect to QC rundown, which can be separated into an early fast (<2 min) and a later slow component (Reid et al., 1999), the chronic stimulations resulted in >100% transformation of the

early component and <100% transformation of the late component in both muscles. Several factors may have contributed to such imprecise transformation. The chronic stimulus patterns may have differed too much from the natural activity patterns of SOL-MNs and EDL-MNs. The duration of chronic stimulation may have been too short. Fast and slow MNs or muscle fibers may possess intrinsic properties that prevent complete transformation. However, because the processes responsible for the two components of QC rundown are unclear, further speculation seems unwarranted at this time.

The transformation of physiological properties observed here was much more pronounced than the fast to slow transformation of structural features at EDL-NMJs observed previously (Wærhaug and Lømo, 1994). Endogenous fast nerve impulse activity, which was present in previous experiments but blocked by TTX in the present experiments, may account for the difference. Alternatively, structural characteristics, such as the number of terminal varicosities, may be more resistant to activity-dependent modulation than the functional properties studied here. For example, when transplanted onto denervated SOL muscles, fast fibular nerve axons form new NMJs of slow appearance when reinnervating sites of the original slow NMJs but of fast appearance when innervation occurs ectopically, suggesting that postsynaptic structures at preformed NMJs are relatively rigid (Wærhaug and Lømo, 1994).

Intrinsic muscle differences clearly restrict the range for activity pattern-induced transformation of contractile properties in rat EDL or SOL muscles. For example, cross-reinnervation, muscle cross-transplantation, or slow pattern stimulation may double the duration of twitch time to peak of rat EDL muscles but not triple it, which would have been required to match the slower twitch of normal SOL muscles (Close, 1969; Gutmann and Carlson, 1975; Eken and Gundersen, 1988; Westgaard and Lømo, 1988). Conversely, cross-reinnervation or fast pattern stimulation may double the intrinsic maximum shortening velocity (V_{max}) of rat SOL muscles but not triple it to match the faster shortening speed of normal EDL muscles (Close, 1969; Eken and Gundersen, 1988). Similarly, fast-pattern stimulation maintains expression of type 2B myosin heavy chain in EDL but cannot induce it in SOL (Ausoni et al., 1990). This probably accounts for the incomplete transformation of intrinsic V_{max} in such studies. Thus, rat SOL and EDL muscles can adapt their contractile properties within intrinsically different but partially overlapping adaptive ranges (Westgaard and Lømo, 1988). Comparable adaptive ranges may similarly restrict adjustment of release properties to imposed impulse patterns at rat SOL-NMJs and EDL-NMJs.

In summary, chronic stimulation with appropriate stimulus patterns can almost completely transform the transmitter release properties of fast and slow NMJs without affecting vesicle RT. These transformations depend on the activity patterns in the NMJs rather than in the parent MN cell bodies and involve adjustments of the ratio of QC to vesicle pool size. Thus, fast and slow NMJs in the rat display long-term activity-dependent plasticity that may fine-tune their transmitter release properties to prevailing firing patterns of the motoneurons in adult life.

References

Ausoni S, Gorza L, Schiaffino S, Gundersen K, Lømo T (1990) Expression of myosin heavy chain isoforms in stimulated fast and slow rat muscles. J Neurosci 10:153–160.

Awad SS, Lightowlers RN, Young C, Chrzanowska-Lightowlers ZMA, Lømo T, Slater CR (2001) Sodium channel mRNAs at the neuromuscular junction: distinct patterns of accumulation and effects of muscle activity. J Neurosci 21:8456–8463.

Barry JA, Ribchester RR (1995) Persistent polyneuronal innervation in partially denervated rat muscle after reinnervation and recovery from prolonged nerve conduction block. J Neurosci 15:6327–6339.

Barstad JAB (1962) Presynaptic effects of the neurotransmitter. Experentia 18:579–580.

Betz WJ, Bewick GS (1992) Optical analysis of synaptic vesicle recycling at the frog neuromuscular junction. Science 255:200–203.

Betz WJ, Bewick GS (1993) Optical monitoring of transmitter release and synaptic vesicle recycling at the frog neuromuscular junction. J Physiol (Lond) 460:287–309.

Campenot RB (1994) NGF and the local control of nerve terminal growth. J Neurobiol 25:599–611.

Campenot RB, Eng H (2000) Protein synthesis in axons and its possible functions. J Neurocytol 29:793–798.

Cangiano A, Lutzemberger L (1980) Normal EDL and diaphragm muscles differ in their sensitivity to tetrodotoxin. Acta Physiol Scand 108:205–207.

Close R (1969) Dynamic properties of fast and slow skeletal muscles of the rat after nerve cross-union. J Physiol (Lond) 204:331–346.

Copray S, Kernell D (2000) Neurotrophins and trk-receptors in adult rat spinal motoneurons: differences related to cell size but not to "slow/fast" specialization. Neurosci Lett 289:217–220.

Czeh G, Gallego R, Kudo N, Kuno M (1978) Evidence for the maintenance of motoneurone properties by muscle activity. J Physiol (Lond) 281:239–252.

Delp MD, Pette D (1994) Morphological changes during fiber type transitions in low-frequency-stimulated rat fast-twitch muscle. Cell Tissue Res 277:363–371.

Deschenes MR, Maresh CM, Crivello JF, Armstrong LE, Kramer WJ, Covault J (1993) The effects of exercise training of different intensities on neuromuscular junction morphology. J Neurocytol 22:603–615.

Eken T, Gundersen K (1988) Electrical stimulation resembling normal motor-unit activity: effects on denervated fast and slow rat muscles. J Physiol (Lond) 402:651–669.

Fahim MA, Holley JA, Robbins N (1984) Topographic comparison of neuromuscular junctions in mouse slow and fast twitch muscles. Neuroscience 13:227–235.

Fengler BT, Lnenicka GA (2002) Activity-dependent plasticity of calcium clearance from crayfish motor axons. J Neurophysiol 87:1625–1628.

Funakoshi H, Belluardo N, Arenas E, Yamamoto Y, Casabona A, Persson H, Ibáñez CF (1995) Muscle-derived neurotrophin-4 as an activity-dependent trophic signal for adult motor neurons. Science 268:1495–1499.

Gertler RA, Robbins N (1978) Differences in neuromuscular transmission in red and white muscles. Brain Res 142:160–164.

Gorza L, Gundersen K, Lømo T, Schiaffino S, Westgaard RH (1988) Slow-to-fast transformation of denervated soleus muscle by chronic high-frequency stimulation in the rat. J Physiol (Lond) 402:627–649.

Gutmann E, Carlson BM (1975) Contractile and histochemical properties of regenerating cross-transplanted fast and slow muscles in the rat. Pflügers Arch 353:227–239.

Hennig R, Lømo T (1985) Firing patterns of motor units in normal rats. Nature 314:164–166.

Hong SJ, Lnenicka GA (1993) Long-term changes in the neuromuscular synapses of a crayfish motoneuron produced by calcium influx. Brain Res 605:121–127.

Hong SJ, Lnenicka GA (1995) Activity-dependent reduction in voltage-dependent calcium current in a crayfish motoneuron. J Neurosci 15:3539–3547.

Jawaid S (2000) Differential changes in neuromuscular junction morphology after divergence of activity pattern in rat slow and fast skeletal muscles. PhD thesis, University of Aberdeen.

Katz B, Thesleff S (1957) On the factors which determine the amplitude of the "miniature" end-plate potential. J Physiol (Lond) 137:267–278.

Kernell D, Eerbeek O, Verhey BA, Donselaar Y (1987) Effects of physiological amounts of high- and low-rate chronic stimulation on cat's fast muscle. 1. Speed- and force-related propertiers. J Neurophysiol 58:598–613.

Kugelberg E, Lindegren B (1979) Transmission and contraction fatigue of rat motor units in relation to succinate dehydrogenase activity of motor unit fibres. J Physiol (Lond) 288:285–300.

Liley AW (1956) An investigation of spontaneous activity at the neuromuscular junction of the rat. J Physiol (Lond) 132:650–666.

Lnenicka GA, Atwood HL (1985) Age-dependent long-term adaptation of

crayfish phasic motor axon synapses to altered activity. J Neurosci 5:459–467.

Lnenicka GA, Atwood HL, Marin L (1986) Morphological transformation of synaptic terminals of a phasic motorneuron by long-term tonic stimulation. J Neurosci 6:2252–2258.

Lnenicka GA, Arcaro KF, Calabro JM (1998) Activity-dependent development of calcium regulation in growing motor axons. J Neurosci 18:4966–4972.

Lømo T, Rosenthal J (1972) Control of ACh sensitivity by muscle activity in the rat. J Physiol (Lond) 221:493–513.

Lømo T, Westgaard RH, Dahl HA (1974) Contractile properties of muscle: control by pattern of muscle activity in the rat. Proc R Soc Lond B Biol Sci 187:99–103.

Martin AR (1955) A further study of the statistical composition of the end-plate potential. J Physiol (Lond) 130:114–122.

McLachlan EM, Martin AR (1981) Non-linear summation of end-plate potentials in the frog and the mouse. J Physiol (Lond) 311:307–324.

Mills RG, Bray JJ (1979) A slow-release technique for inducing prolonged paralysis by tetrodotoxin. Pflügers Arch 383:67–70.

Pasino E, Buffelli M, Arancio O, Busetto G, Salviati A, Cangiano A (1996) Effects of long-term conduction block on membrane properties of reinnervated and normally innervated rat skeletal muscle. J Physiol (Lond) 497:457–472.

Plomp JJ, van Kempen GTH, Molenaar PC (1992) Adaptation of quantal content to decreased postsynaptic sensitivity at single endplates in α-bungarotoxin-treated rats. J Physiol (Lond) 458:487–499.

Reid B, Slater CR, Bewick GS (1999) Synaptic vesicle dynamics in rat fast and slow motor nerve terminals. J Neurosci 19:2511–2521.

Salmons S, Henriksson J (1981) The adaptive response of skeletal muscle to increased use. Muscle Nerve 4:94–105.

Salmons S, Vrbova G (1969) The influence of activity on some contractile characteristics of mammalian fast and slow muscles. J Physiol (Lond) 201:535–549.

Sterz R, Pagala M, Peper K (1983) Postjunctional characteristics of the end-plates in mammalian fast and slow muscles. Pflügers Arch 398:48–54.

Tsujimoto T, Kuno M (1988) Calcitonin gene-related peptide prevents disuse-induced sprouting of rat motor nerve terminals. J Neurosci 8:3951–3957.

Wærhaug O (1992) Postnatal development of rat motor nerve terminals. Anat Embryol 185:115–123.

Wærhaug O, Lømo T (1994) Factors causing different properties at neuromuscular junctions in fast and slow rat skeletal muscles. Anat Embryol 190:113–125.

Wang XH, Berninger B, Poo MM (1998) Localized synaptic actions of neurotrphin-4. J Neurosci 18:4985–4992.

Westgaard RH, Lømo T (1988) Control of contractile properties within adaptive ranges by patterns of impulse activity in the rat. J Neurosci 8:4415–4426.

Windisch A, Gundersen K, Szabolcs MJ, Gruber H, Lømo T (1998) Fast to slow transformation of denervated and electrically stimulated rat muscle. J Physiol (Lond) 510:623–632.

Wood SJ, Slater CR (1997) The contribution of postsynaptic folds to the safety factor for neuromuscular transmission in rat fast- and slow-twitch muscles. J Physiol (Lond) 500:165–176.

Wood SJ, Slater CR (2001) Safety factor at the neuromuscular junction. Prog Neurobiol 64:393–429.